

# Investigation on the Long-Term Stability of $\text{AlO}_x/\text{SiN}_y\text{:H}$ and $\text{SiN}_y\text{:H}$ Passivation Layers During Illuminated Annealing at Elevated Temperatures

Fabian Geml<sup>1</sup>[\[https://orcid.org/0000-0002-2803-5390\]](https://orcid.org/0000-0002-2803-5390), Melanie Mehler<sup>1</sup>[\[https://orcid.org/0000-0002-0557-6290\]](https://orcid.org/0000-0002-0557-6290), Sarah Sanz<sup>1</sup>[\[https://orcid.org/0009-002-6530-0963\]](https://orcid.org/0009-002-6530-0963), Axel Herguth<sup>1</sup>[\[https://orcid.org/0000-0003-1079-1179\]](https://orcid.org/0000-0003-1079-1179), and Giso Hahn<sup>1</sup>[\[https://orcid.org/0000-0001-8292-1281\]](https://orcid.org/0000-0001-8292-1281)

<sup>1</sup> University Konstanz, Germany

**Abstract.** Most crystalline Si based solar cells, e.g. passivated emitter and rear cells, rely on  $\text{SiN}_y\text{:H}$  and  $\text{AlO}_x/\text{SiN}_y\text{:H}$  passivation layers. In this work, the long-term behavior of minority charge carrier lifetime in such symmetrically passivated samples during illuminated annealing at elevated temperatures is investigated by means of photoconductance decay based lifetime measurements, corona charging and capacitance voltage measurements. Thereby,  $\text{AlO}_x$  layers, which are known to reduce H in-diffusion due to their barrier properties, deposited by atmospheric pressure chemical vapor deposition as well as by atomic layer deposition were considered enabling a comparison of different deposition techniques. The frequently published behavior of the bulk related degradation could be confirmed and the qualitative correlation between maximum defect density and the changing total amount of H in the Si bulk due to the barrier properties of the individual layers dielectric layers could be shown. Furthermore, for the subsequently observed degradation accelerated by a treatment at higher temperatures, literature indicates degradation to be caused by surface related degradation. Investigations on field effect passivation during degradation by means of corona charging and CV measurements showed a large drop in fixed negative charges in the passivation layer stacks.

**Keywords:** Degradation, Surface passivation, Crystalline silicon

## 1. Introduction

Bulk related degradation (BRD) phenomena, such as light- and elevated temperature-induced degradation (LeTID), can reduce bulk minority charge carrier lifetime and thereby affect the efficiency of Si solar cells. However, the effective minority charge carrier lifetime  $\tau_{\text{eff}}$  may suffer from surface related degradation (SRD) as well [1], [2]. Literature indicates that SRD can occur in samples passivated by  $\text{SiN}_y\text{:H}$  and  $\text{AlO}_x/\text{SiN}_y\text{:H}$  [2] – both passivation layer systems found in passivated emitter and rear cells (PERC). For both, LeTID and SRD, it is known that properties of the passivation layer can influence the kinetics of LeTID [3] and SRD [4]. In this work, short- and long-term stability of  $\tau_{\text{eff}}$  in samples passivated by  $\text{SiN}_y\text{:H}$  and  $\text{AlO}_x/\text{SiN}_y\text{:H}$  during illuminated annealing at elevated temperatures is investigated.  $\text{AlO}_x$  layers from two different deposition tools, atmospheric pressure chemical vapor deposition (APCVD) and atomic layer deposition (ALD), are considered to check whether different  $\text{AlO}_x$  layer microstructures have an impact on degradation kinetics as already indicated in a previous study [5].

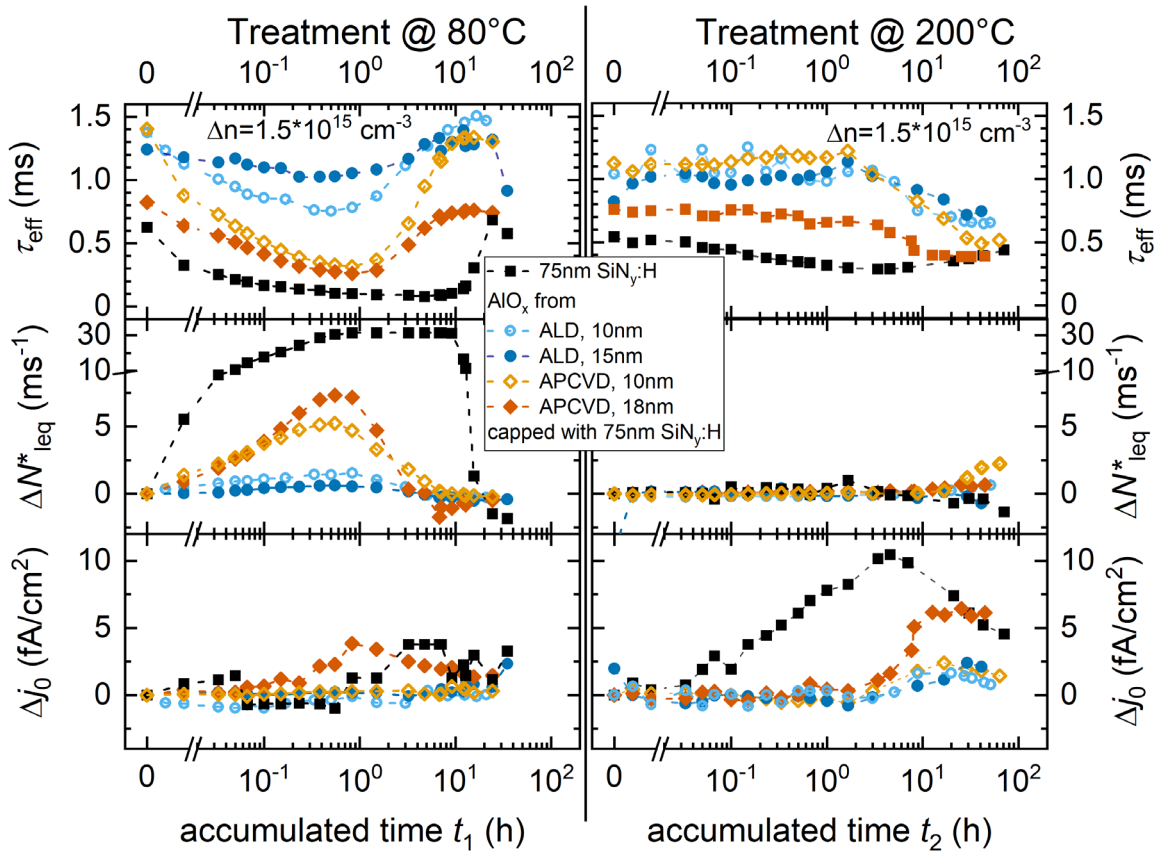
## 2. Experimental

For the degradation experiments  $\sim 1 \text{ } \Omega\text{cm}$  B-doped FZ-Si wafers serve as base material. After

an HF etching step, 5-18 nm  $\text{AlO}_x$  is deposited on both sides by two different deposition techniques, APCVD at 590°C and ALD at 300°C, except for reference samples. All samples are then coated on both sides with 75 nm  $\text{SiN}_y\text{:H}$  via plasma-enhanced chemical vapor deposition and subsequently fired at a sample peak firing temperature of  $T_{\text{sample,peak}} = 800^\circ\text{C}$ . LeTID related degradation and regeneration is carried out at 80°C and 0.9(1) suns. After reaching a maximum in  $\tau_{\text{eff}}$ , indicating that SRD starts to become dominant, treatment temperature is increased to 200°C to accelerate this second degradation.  $\tau_{\text{eff}}$  is determined at room temperature using photoconductance decay (PCD) evaluated at an excess charge carrier density  $\Delta n = 0.1 p_0 \approx 1.5 \cdot 10^{15} \text{ cm}^{-3}$ , with  $p_0$  being the base doping. From PCD measurements, the lifetime equivalent maximum defect density ( $\Delta n \rightarrow 0$ )  $\Delta N_{\text{leq}}^*$  is calculated as described in [6], [7]. Additionally, the surface saturation current density  $j_0$  is determined. The evaluation of  $j_0$  during both, BRD and SRD was performed by the  $j_0$  difference analysis according to [7].

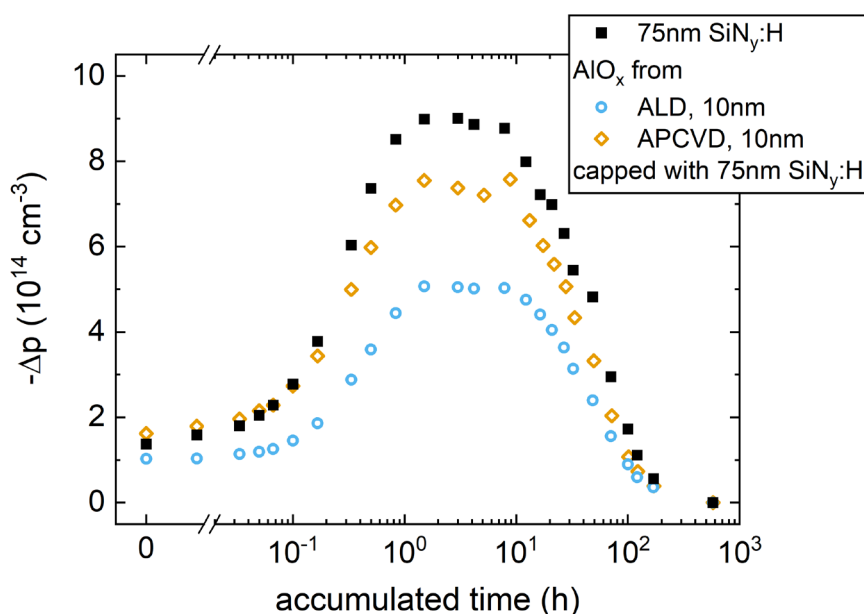
For the investigation of the passivation mechanism during SRD, the alternating PCD measurement and applying of corona charging (CC) are performed at two specific times, directly at the beginning of the temperature treatment at higher temperature ( $t_{2,\text{initial}}$ ) and at the  $\tau_{\text{eff}}$  minimum of SRD ( $t_{2,\text{min}}$ ). In addition, the fixed charge density  $Q_f$  in the  $\text{SiN}_y\text{:H}$  and  $\text{AlO}_x/\text{SiN}_y\text{:H}$  layers is determined by capacitance voltage (CV) measurements directly after firing and at the  $\tau_{\text{eff}}$  minimum of SRD. For CV measurements, Al was evaporated on one side of the samples followed by production of laser fired contacts (LFC). The evaluation of the CV data is performed according to [8] via the determination of the slope of the  $1/C^2$  curve. The H content in the Si bulk is analyzed via resistivity measurements to determine the amount of acceptor-hydrogen pairs according to [9].

### 3. Results and Discussion



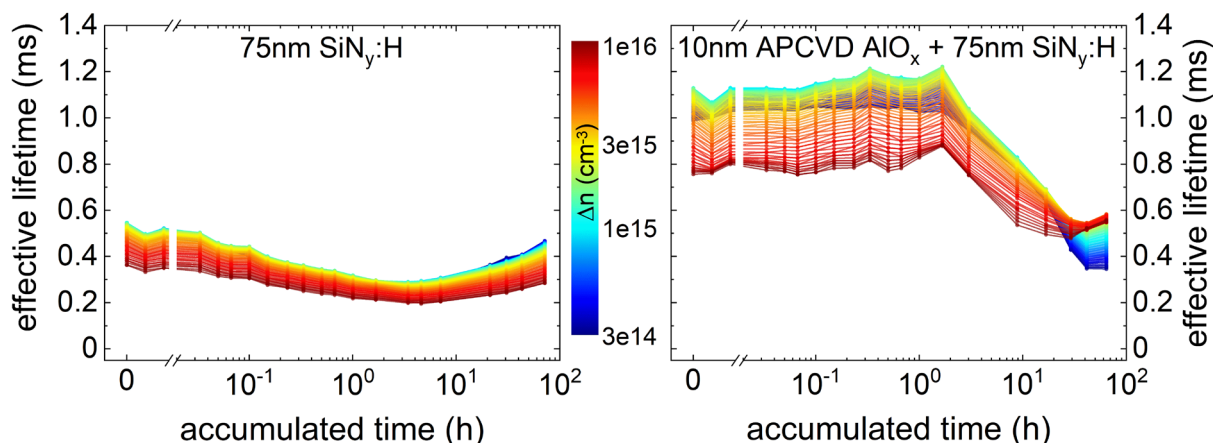
**Figure 1.** Measured  $\tau_{\text{eff}}$  (top) and resulting  $\Delta N_{\text{leq}}^*$  (middle) and change in  $j_0$  (bottom) compared to initial values versus accumulated time for  $\text{SiN}_y\text{:H}$  and  $\text{AlO}_x/\text{SiN}_y\text{:H}$  passivated samples. To trigger degradation and regeneration related to LeTID, samples are first illuminated at 80°C (left) and subsequently at 200°C for accelerated study of SRD (right).

Fig. 1 shows the measured  $\tau_{\text{eff}}$ , the resulting  $\Delta N_{\text{leq}}^*$ , and change in  $j_0$  values for the differently passivated samples. As expected, the progression of  $\tau_{\text{eff}}$  and  $\Delta N_{\text{leq}}^*$  values during illuminated annealing at 80°C shows a degradation and regeneration behavior which can be attributed to the LeTID defect. The occurrence of a BRD is indicated by the fact that  $j_0$  stays nearly constant during degradation. During degradation at 80°C, the samples with  $\text{AlO}_x$  layer show lower  $\Delta N_{\text{leq}}^*$  values compared to the sample with only  $\text{SiN}_y\text{:H}$ . With LeTID known to scale with the bulk H content, this behavior can be attributed to the barrier properties of the  $\text{AlO}_x$  layer, known to reduce in-diffusion of H [10], [11]. Indeed, a supplemental study on BH-pair formation confirms this reduced H content, see Fig. 2.



**Figure 2.** Change in hole concentration  $-\Delta p$  versus accumulated time during dark anneal at 220°C for the differently passivated samples (fired).

Compared to ALD  $\text{AlO}_x$ , APCVD  $\text{AlO}_x$  shows barrier properties which are not as strong. After switching the treatment temperature to 200°C, the differently passivated samples suffer from a second degradation, whereby the samples with  $\text{AlO}_x/\text{SiN}_y\text{:H}$  stacks show a significantly delayed degradation compared to the  $\text{SiN}_y\text{:H}$  reference. The steady increase in  $j_0$  of the  $\text{SiN}_y\text{:H}$  passivated sample suggests that this second degradation is related to surface passivation (SRD). A slight increase in  $j_0$  is also observable for the  $\text{AlO}_x/\text{SiN}_y\text{:H}$  stacks but especially for the thinner  $\text{AlO}_x$  samples only to a very limited extent. Considering  $\Delta N_{\text{leq}}^*$ , especially for the sample group with thinner APCVD  $\text{AlO}_x$ , it can be observed that something seems to change in the bulk for >20 h. This can also be confirmed in Fig. 3 (right). The injection-resolved lifetime curves show a reverse behavior (lower lifetimes at low injection) for  $t > 20$  h, which can undoubtedly be assigned to a BRD. So far, it is not clear what triggers this phenomenon.



**Figure 3.** Injection resolved  $\tau_{\text{eff}}$  over accumulated time of the sample with  $\text{SiN}_y\text{:H}$  (left) and of a sample with APCVD  $\text{AlO}_x/\text{SiN}_y\text{:H}$  (right) during degradation at  $200^\circ\text{C}$  (right).

Focusing on the surface, the behavior during CC of the samples is investigated, presented in Fig. 4, where the measured  $\tau_{\text{eff}}$  is shown depending on charging time. At the beginning of SRD, the respective  $\tau_{\text{eff}}$  minimum of the  $\text{AlO}_x/\text{SiN}_y\text{:H}$  stacks is almost at the same level. Compared to the  $\text{SiN}_y\text{:H}$  sample, the samples with  $\text{AlO}_x/\text{SiN}_y\text{:H}$  stacks show a higher minimum. However, a different behavior can be observed at the minimum in  $\tau_{\text{eff}}$  of the following treatment at  $200^\circ\text{C}$  (Fig. 4, right). The minima of the  $\text{AlO}_x/\text{SiN}_y\text{:H}$  stacks are on a similar or even slightly higher level than at  $t_{2,\text{initial}}$ , but the CC time has decreased tremendously. Conversely, it can be observed for the  $\text{SiN}_y\text{:H}$  sample that the  $\tau_{\text{eff}}$  minimum is slightly decreased and the corona charging time is very similar compared to  $t_{2,\text{initial}}$ . Note that a rather uncharged surface also leads to the fact that lifetime may not be described by an injection-independent  $j_0$  value. This may explain the drop in  $j_0$  during the second degradation (see Fig. 1, right) for the thinner  $\text{AlO}_x$  layer stacks.

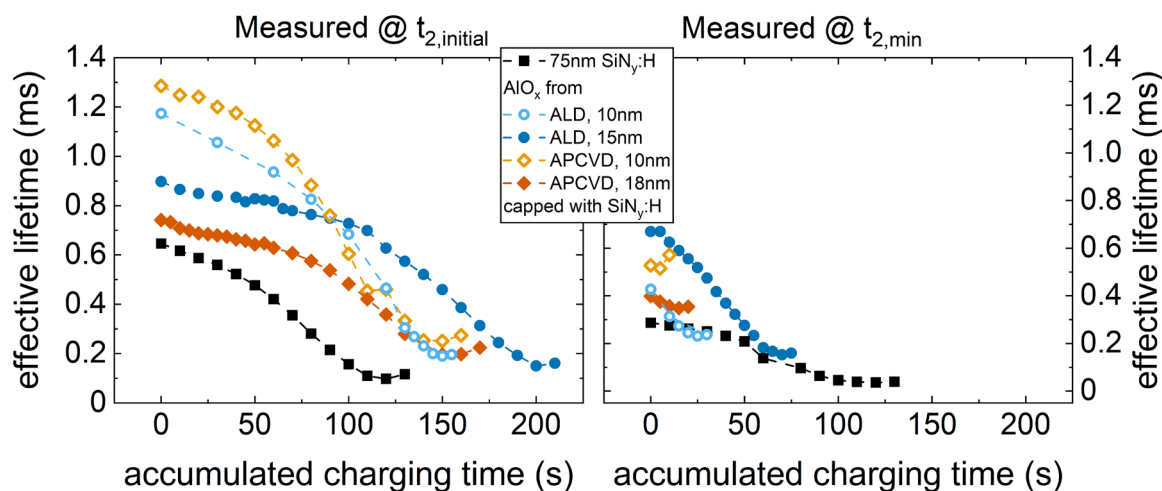


**Figure 4.** Corona charging time at the  $\tau_{\text{eff}}$  minimum of the different samples with  $\text{SiN}_y\text{:H}$  layer or  $\text{AlO}_x/\text{SiN}_y\text{:H}$  layer stacks at the beginning (left) and at the minimum in  $\tau_{\text{eff}}$  of the second degradation at  $200^\circ\text{C}$  (right). Negative charging for  $\text{SiN}_y\text{:H}$ , positive charging for  $\text{AlO}_x/\text{SiN}_y\text{:H}$ .

Thus, SRD in the  $\text{SiN}_y\text{:H}$  passivated sample could be explained by the decrease in chemical surface passivation quality, whereas the second degradation, between  $\sim 1\text{-}10$  h at  $200^\circ\text{C}$ , in  $\text{AlO}_x/\text{SiN}_y\text{:H}$  passivated samples, seems to be related to a decrease in field effect passivation. It is remarkable that despite the strongly different extent of initial BRD, both, samples with ALD and APCVD  $\text{AlO}_x$  layers, show a very similar course during the second degradation.

For a comparison of the CC measurements, the CC duration until reaching the  $\tau_{\text{eff}}$  minimum is shown for the differently passivated samples in Fig. 5 (left). In addition, CV measurements are applied to measure the absolute fixed charge density which is shown in Fig. 5 (right). Samples with  $\text{AlO}_x/\text{SiN}_y:\text{H}$  layers show a decline of negative fixed charges during SRD measured by CC as well as by CV. However, the quantitative amount measured by CV cannot be directly compared with the corona charging time, especially for APCVD  $\text{AlO}_x$  interlayers, which may be due to the differences in the layer microstructure. While the CC time of the  $\text{SiN}_y:\text{H}$  passivated samples does not change significantly during SRD, the CV measurements show that there is a slight increase in positive fixed charge density. There is thus a net decline of negative charge density or net increase of positive charge density during SRD independent of the passivation type. However, which of these is the case cannot be clearly assigned by the CV measurement. This allows the hypothesis to be made that the net fixed charge is involved in the SRD and opens the further question whether the positively charged H species plays a key role in SRD.

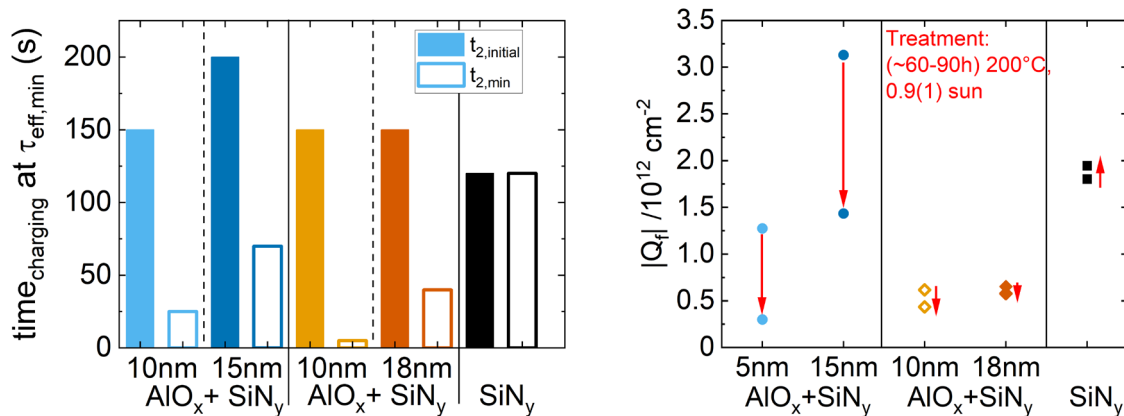


**Figure 5.** (Left) Corona charging time required to reach the  $\tau_{\text{eff}}$  minimum (in Fig. 4) of the different samples with  $\text{SiN}_y:\text{H}$  layer or  $\text{AlO}_x/\text{SiN}_y:\text{H}$  layer stacks at the beginning (filled) and at the minimum of the second degradation (unfilled). (Right) Absolute fixed charge density  $|Q_f|$  from CV measurements of the different samples with  $\text{SiN}_y:\text{H}$  layer or  $\text{AlO}_x/\text{SiN}_y:\text{H}$  layer stacks directly after firing and after reaching the minimum of the second degradation. Blue colours: ALD  $\text{AlO}_x$ , orange colours: APCVD  $\text{AlO}_x$ .

## 4. Conclusion

It could be shown that  $\text{AlO}_x$  layers from ALD and APCVD both serve as a barrier layer for H during firing. Since the  $\Delta N_{\text{ieq}}^*$  and  $-\Delta p$  values of the ALD  $\text{AlO}_x/\text{SiN}_y:\text{H}$  passivated samples are lower than those of the APCVD  $\text{AlO}_x/\text{SiN}_y:\text{H}$  passivated samples, it is concluded that the ALD  $\text{AlO}_x$  layer has a stronger barrier effect and/or is a less effective source of H. This also confirms a correlation between  $\Delta N_{\text{ieq}}^*$  and H amount for LeTID. The second degradation for the  $\text{SiN}_y:\text{H}$  passivated samples could be attributed to SRD by the steady increase of  $j_0$  and by the injection resolved lifetime. On the other hand, the  $\text{AlO}_x/\text{SiN}_y:\text{H}$  passivated samples with ALD and thin APCVD  $\text{AlO}_x$  layers show only a slight increase in  $\Delta j_0$  and in addition the thin APCVD  $\text{AlO}_x$  layer sample group showed a reverse dependence in the injection-resolved lifetimes for >10 h at 200°C, indicating another and yet unknown BRD effect. From the CC and CV measurements, a decline of negative fixed charges in the  $\text{AlO}_x/\text{SiN}_y:\text{H}$  layers could be observed during SRD while in the  $\text{SiN}_y:\text{H}$  layer there is a slight increase in positive fixed charge density.

## Data availability statement

The data that support the findings of this study are available from the corresponding author upon reasonable request.

## Author contributions

**F. Geml:** conceptualization, project administration, supervision, validation, writing – original draft, writing – review & editing; **M. Mehler:** formal analysis, investigation, validation, visualization, conceptualization, writing – original draft, writing – review & editing; **S. Sanz:** investigation; **A. Herguth:** software, validation, writing – review & editing; **G. Hahn:** funding acquisition, project administration, resources, supervision, writing – review & editing.

## Competing interests

The authors declare that they have no competing interests.

## Funding

Part of this work was funded by German Federal Ministry for Economic Affairs and Climate Action under contract numbers FKZ 03EE1051C and FKZ 03EE1102C. The content is the responsibility of the authors.

## References

1. P. E. Gruenbaum, R. A. Sinton, R. M. Swanson, "Light-induced degradation at the silicon/silicon dioxide interface," *Applied Physics Letters*, vol.52, pp. 1407–1409, 1988, doi: <https://doi.org/10.1063/1.99130>.
2. D. Sperber, A. Graf, D. Skorka, A. Herguth, G. Hahn, "Degradation of surface passivation on crystalline silicon and its impact on light-induced degradation experiments," *IEEE Journal of Photovoltaics*, vol.7, pp. 1627-1634, 2017, <https://doi.org/10.1109/JPHOTOV.2017.2755072>.
3. F. Kersten, P. Engelhart, H. C. Ploigt, A. Stekolnikov, T. Lindner, F. Stenzel, M. Bartsch, A. Szpeth, K. Petter, J. Heitmann, J.W. Müller, "Degradation of multicrystalline silicon solar cells and modules after illumination at elevated temperature," *Solar Energy Materials and Solar Cells*, vol.142, pp. 83-86, 2015, doi: <https://doi.org/10.1016/j.solmat.2015.06.015>.
4. D. Sperber, A. Schwarz, A. Herguth, G. Hahn, "Bulk and surface-related degradation in lifetime samples made of Czochralski silicon passivated by plasma-enhanced chemical vapor deposited layer stacks," *Physica Status Solidi (a)*, vol.215, pp. 1800741, 2018, doi: <https://doi.org/10.1002/pssa.201800741>.
5. M. Mehler, F. Geml, A. Schmid, A. Zuschlag, G. Hahn, "Effect of different AlO<sub>x</sub> passivation layers deposited by APCVD and ALD on LeTID", in *Proc. 8<sup>th</sup> WCPEC, 2022*, pp. 142-144.
6. A. Herguth, "On the lifetime-equivalent defect density: properties, application, and pitfalls," *IEEE Journal of Photovoltaics*, vol.9, no.5, pp. 1182-1194, 2019, doi: <https://doi.org/10.1109/JPHOTOV.2019.2922470>.
7. A. Herguth, J. Kamphues, "On the impact of bulk lifetime on the quantification of recombination at the surface of semiconductors," *IEEE Journal of Photovoltaics*, submitted, 2023. doi: <https://doi.org/10.1109/JPHOTOV.2023.3291453>.
8. D. K. Schroder, "Carrier and Doping Density," in *Semiconductor Material and Device characterization* (John Wiley & Sons, 2015) third ed. New Jersey, 2015, ch. 2, pp. 61-68.
9. A. Herguth, C. Winter, "Methodology and error analysis of direct resistance measurements used for the quantification of boron–hydrogen pairs in crystalline silicon," *IEEE Journal of Photovoltaics*, vol.11, no.4, pp. 1059–1068, Jul., 2021, doi: <https://doi.org/10.1109/JPHOTOV.2021.3074463>.

10. A. Schmid, C. Fischer, D. Skorka, A. Herguth, C. Winter, A. Zuschlag, G. Hahn, "On the role of  $\text{AlO}_x$  thickness in  $\text{AlO}_x/\text{SiN}_y\text{:H}$  layer stacks regarding light- and elevated temperature-induced degradation and hydrogen diffusion in c-Si," *IEEE Journal of Photovoltaics*, vol.11, no.4, pp. 967-973, 2021, doi: <https://doi.org/10.1109/JPHOTOV.2021.3075850>.
11. L. Helmich, D. C. Walter, D. Bredemeier, J. Schmidt, "Atomic-layer-deposited  $\text{Al}_2\text{O}_3$  as effective barrier against the diffusion of hydrogen from  $\text{SiN}_x\text{:H}$  layers into crystalline silicon during rapid thermal annealing," *Physica Status Solidi RRL*, vol.14, p. 2000367, 2020, doi: <https://doi.org/10.1002/pssr.202000367>.